2009

An Investigation of the First-Order Mechanics of Polygonal Fault Networks of Utopia Planitia, Mars

Fariha Islam
University of Massachusetts Amherst

AN INVESTIGATION OF THE FIRST-ORDER MECHANICS OF POLYGONAL FAULT NETWORKS OF UTOPIA PLANITIA, MARS

A Thesis Presented

By

FARIHA ISLAM

Submitted to the Graduate School of the
University of Massachusetts Amherst in partial fulfillment
of the requirements for the degree of

MASTER OF SCIENCE

February 2009

Department of Geosciences

AN INVESTIGATION OF THE FIRST-ORDER MECHANICS OF POLYGONAL FAULT NETWORKS OF UTOPIA PLANITIA, MARS

A Thesis Presented

By

FARIHA ISLAM

Approved as to style and content by:

_____
George E. McGill, Chair

_____
Michele L. Cooke, Member

_____
Christopher D. Condit, Member

_____
Michael L. Williams, Department Head
Department of Geosciences

ACKNOWLEDGEMENTS

I would like to thank my advisors, George E. McGill and Michele L. Cooke, for their guidance and continued support. I would also like to extend my gratitude to Christopher D. Condit for his assistance as a member of my thesis committee. Many thanks to Eileen McGowan and Don Sluter for their aid with my technical and software inquiries. I want to thank Josh Banfield of Arizona State University for providing me with the THEMIS mosaic data used in this study. Finally, a special thank you to my family and friends for their encouragement and kind words throughout this endeavor.

TABLE OF CONTENTS

Page

LIST OF TABLES

LIST OF FIGURES

CHAPTER 1

INTRODUCTION

Since the first Viking images were sent back from Mars, researchers have been asking the same key questions about the giant polygons of Utopia Planitia: What process(es) created the giant polygons and why are they so large? This paper addresses these still puzzling questions.

CHAPTER 2

GEOLOGIC BACKGROUND

Mars giant polygons

Similar style and scale polygonal terrains are found in both the Northern Lowlands regions of the Acidalia Planitia (45ºN, 15ºW) and Elysium Planitia (36ºN, 256ºW) on Mars. However, this study is confined to Utopia Planitia (49ºN, 233ºW), specifically the southwestern region of the polygonal terrain as defined in Figure 1, due to the available satellite imagery and altimetry for this area. The giant polygons of Utopia Planitia, Mars are characterized by troughs tens of meters deep that define polygonal fault networks that have 1 to 40 km spacing between troughs (Figure 2). A number of hypotheses for their origin have been proposed such as desiccation of water saturated sediments, thermal cooling and contraction in permafrost, cooling of lava, and tectonic deformation. Pechmann [1980] has demonstrated that none of these terrestrial analogs would lead to a satisfactory description of the mechanisms and scales involved. Additionally, these terrestrial polygons have been observed on Mars at the scale at which they occur on Earth (i.e. patterned ground, periglacial-related polygonal ground of the mid-latitudes and columnar basalt).

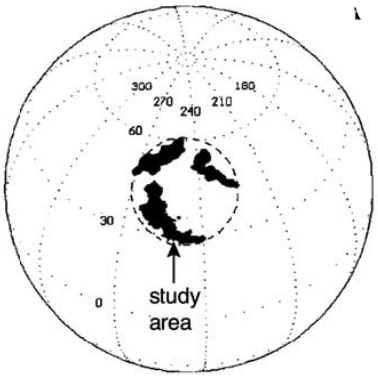

Figure 1: Study area is the southern most expression of the polygonal terrain in the Utopia Basin as mapped by G. McGill [1986].

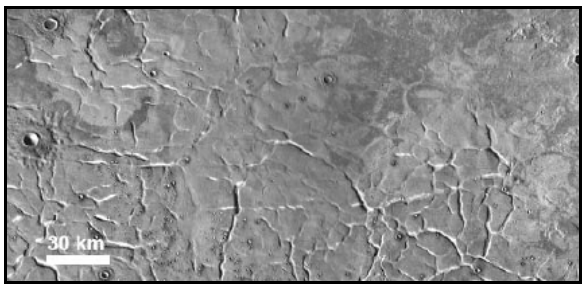

Figure 2: THEMIS Daytime Infrared Mosaic of a region in the Utopia Basin.

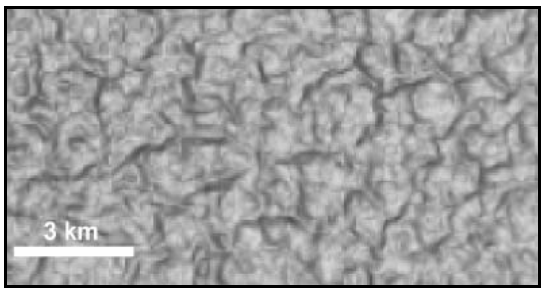

Figure 3: Seismic map of a polygonal network in sediments in the Lower Congo Basin.

North Sea terrestrial polygons

Polygonal fault networks have also been found in layers of mudrocks and chalks beneath oceans in sedimentary basins around the world (Figure 3). These terrestrial polygons were first documented in Lower Tertiary mudrocks from the North Sea Basin

by Cartwright [1984]; 28 basins have currently been identified through 2D and 3D seismic studies to have extensive fault systems defining polygons with diameters up to 3 km. Earth polygonal terrains are located on passive margins in onlap fill units and are generally comprised of very fine-grained sediments [e.g. Cartwright, 1984; Cartwright and Lonergan, 1996; Cartwright and Lonergan, 1997; Lonergan, *et al*., 1998; Cartwright and Dewhurst, 1998; Dewhurst, *et al*., 1999; Gay, *et al*., 2004]. The overlap in scale between the 3 km diameter terrestrial polygons and the 1-40 km diameter giant polygons of Mars suggests that they may have similar origins.

Possible water-laid origin of Utopia units

A number of observations support a water-laid sedimentary origin for the materials within which the giant martian polygons occur. Polygonal terrains occur in the lowest parts of the northern lowland, the most logical places for water to pond and sediments to accumulate if oceans or large lakes did occur [e.g. Lucchitta, *et al*., 1986; McGill, 1989; Smith, *et al*., 1999]. Craters superposed on these terrains are dominantly characterized by fluidized ejecta, generally thought to be due to significant volatile content in the target material [Mouginis-Mark, 1979]. The upper elevation limit for polygonal terrain exposures along the south flank of the Utopia Basin occurs close to an elevation of -4350 meters [Hiesinger and Head, 2000], approximately coinciding with a topographic terrace along the flank of the Utopia Basin that has been interpreted to be a paleoshoreline [Thompson and Head, 1999]. The ancient impact basin of Utopia Planitia [McGill, 1989; Smith, *et al*., 1999] is thought to be covered with sedimentary and volcanic material by Scott and Tanaka [1986]. Luchitta *et al*. [1986] support the material being of sedimentary origin deposited in a standing body of water. Aharonson et al.,

[1998] compared the surface roughness of the Northern Lowlands with other planetary bodies and suggest that certain regions of the Highlands are comparable to terrestrial sedimentary basins.

Similar volcanic sedimentary origins

On Earth, the North Sea polygons form in a sequence of smectite-rich volcanic mudrocks produced from altered volcanic glass [Dewhurst, *et al*., 1999] and may be a possible analog for the martian polygonal terrain materials.

Terrestrial polygon formation and the basis for the investigation

Cartwright and Lonergan [1996] have suggested that the polygonal faults of the North Sea have formed in response to three-dimensional compaction of the fine-grained sediments during burial. The polygonal faults exhibit radial strain patterns in plan view; the deformation is layer bound to the fine-grained stratigraphic units with no evidence of extensional displacement onto basement structures. Cartwright and Lonergan [1996] propose that extension is accommodated by layer-parallel volumetric contraction. Part of the volume reduction due to pore fluid loss is thus accommodated by extensional faulting [Cartwright and Lonergan, 1996; Lonergan, *et al*., 1998]. The fault networks in the terrestrial basins are not caused by any tectonic mechanism as suggested by the lack of displacement onto basement structures. McGill and Hills [1992] also suggested that extensional strain produced the grabens in Utopia Planitia based on a 2D differential compaction model (desiccation shrinkage of wet sediments) with the scale of the giant polygons determined by the topography of the underlying surface instead of a tectonic mechanism. Buczkowski and Cooke [2004] showed that volumetric compaction of sedimentary material over buried craters is a feasible model for the development of

grabens within Utopia. Volumetric contraction seems to accommodate the extensional faulting observed in earth polygonal terrains and the giant martian polygonal terrains and will be further explored in this study.

CHAPTER 3

FAULT CHARACTERIZATION

Analysis of the morphology of the troughs

The morphology of the troughs that define the giant polygons of Utopia has been extensively studied. The troughs, inferred to be a set of normal faults or grabens, have a wide variation in strike orientations which gives rise to the polygonal pattern. Using Viking imagery, Pechmann [1980] described typical polygon forming troughs in the lowlands as long sinuous depressions (200-800m wide, 5-10 km apart and troughs 30-107 m ± 10 deep). He noted that wider troughs have flat floors and steep sides with many troughs exhibiting one or two smooth terraces along sections of the wall attributed to post-faulting modification. He observed that trough intersections are infrequent and for this reason, completely closed polygons are rare. Some troughs narrow and shallow at the end, while some have steep, blunt terminations and others end in gentle ramps. He also observed that circular troughs and pairs of concentric circular troughs are common.

Also using Viking imagery, McGill and Hills [1992] described the areal pattern defined by the troughs as very complex and generally 'polygonal'. McGill's [1989] stratigraphic studies showed that the polygonally fractured material in Utopia was deposited on a land surface with significant topography, including scattered knobs and mesas, fragments of ancient crater rims, and fresh younger craters. Comparing polygonal troughs with relief features on the surface indicated a pattern and spacing of the buried topographic features that corresponded well with the pattern and scale of the troughs [McGill and Hills, 1992]. They correlated circular troughs with buried crater rims and large single knobs or mesas as the loci of major trough source points. The tendency of

knob clusters to be linear or arcuate provided the explanation for similar patterns seen in troughs.

Hiesinger and Head [2000] added to the analysis of the giant polygons using higher resolution Mars Orbiter Camera (MOC) imagery and Mars Orbiter Laser Altimeter (MOLA) datasets. They noted that the troughs are generally broad, graben-like features with variable morphology including symmetric or asymmetric graben wall shape. They observed that a large number of troughs exhibit rounded rims and that the average trough width is about 2 km and the average trough depth is 30m. They found that trough depth tends to increase toward the basin center but that the trough width is not strongly correlated to distance from the center of the basin. They observe that in MOC images wider troughs show morphologic features along the trough walls that can be either interpreted as terraces or products of listric faulting. In MOC images, they observed that trough bottoms generally appear flat and have dunes indicating that the original morphology was later modified by aeolian activity.

The new High Resolution Imaging Science Experiment (HiRISE) images also show the complexity of both symmetric and asymmetric grabens that define the troughs. Figure 4 shows both types of grabens with green arrows pointing to symmetrical type grabens and the red arrows pointing to asymmetrical grabens. Both walls of symmetrical grabens are linear or seem to mirror each while the asymmetrical grabens in Figure 6 displays en-echelon faulting. In Figure 4, this asymmetric graben has one wall that is linear and a complimentary wall that is curvilinear. Both types of grabens are displayed in Figure 5. The asymmetrical grabens display many variations—one wall linear, the

complimentary wall curvilinear or jagged or both walls en-echelon or both walls curvilinear but not symmetrically so.

In the previous papers, researchers refer to terraces, which are generally defined as slump features to further faulted blocks within the troughs. With the greater resolution of the HiRISE dataset, a bulge or ridge-like feature, mirroring the graben wall is observed in some of the troughs (Figure 4-6). The grabens in Figure 6 show that these bulge features also display an asymmetry since they appear adjacent to only one wall of the graben. If these features are common in the polygonal terrain, further analysis using HiRISE imagery may reveal information about the graben formation process and/or post-faulting modification.

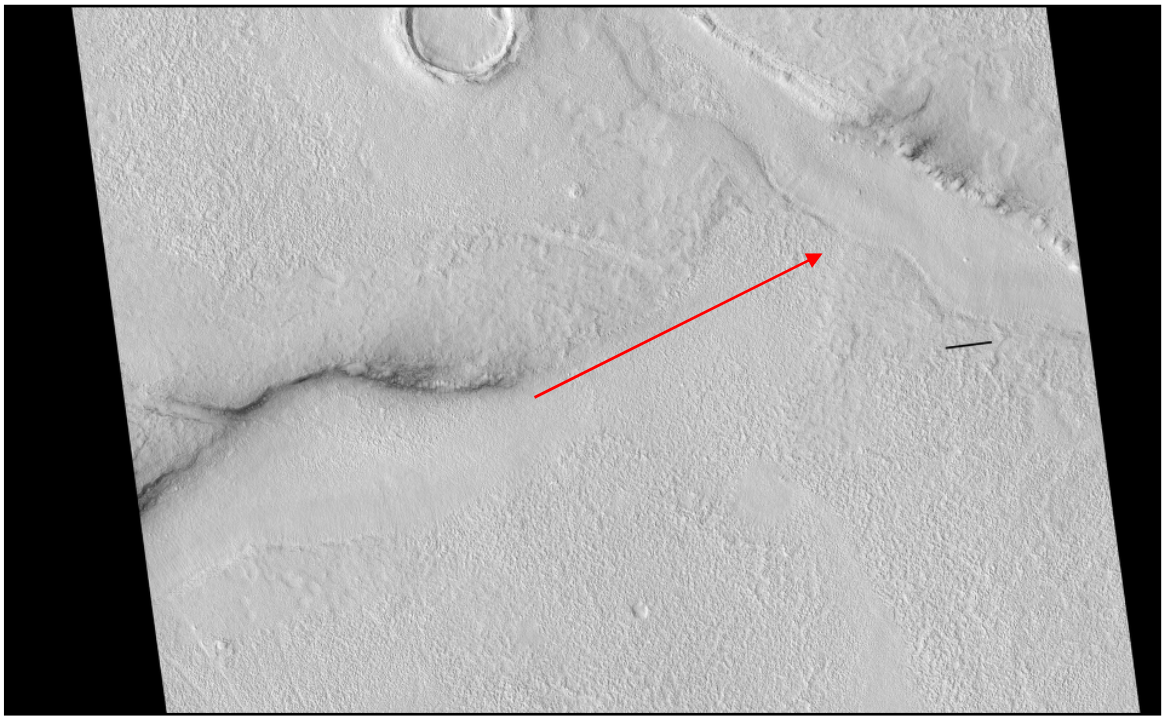

Figure 4: HiRISE image PSP 8504_2195

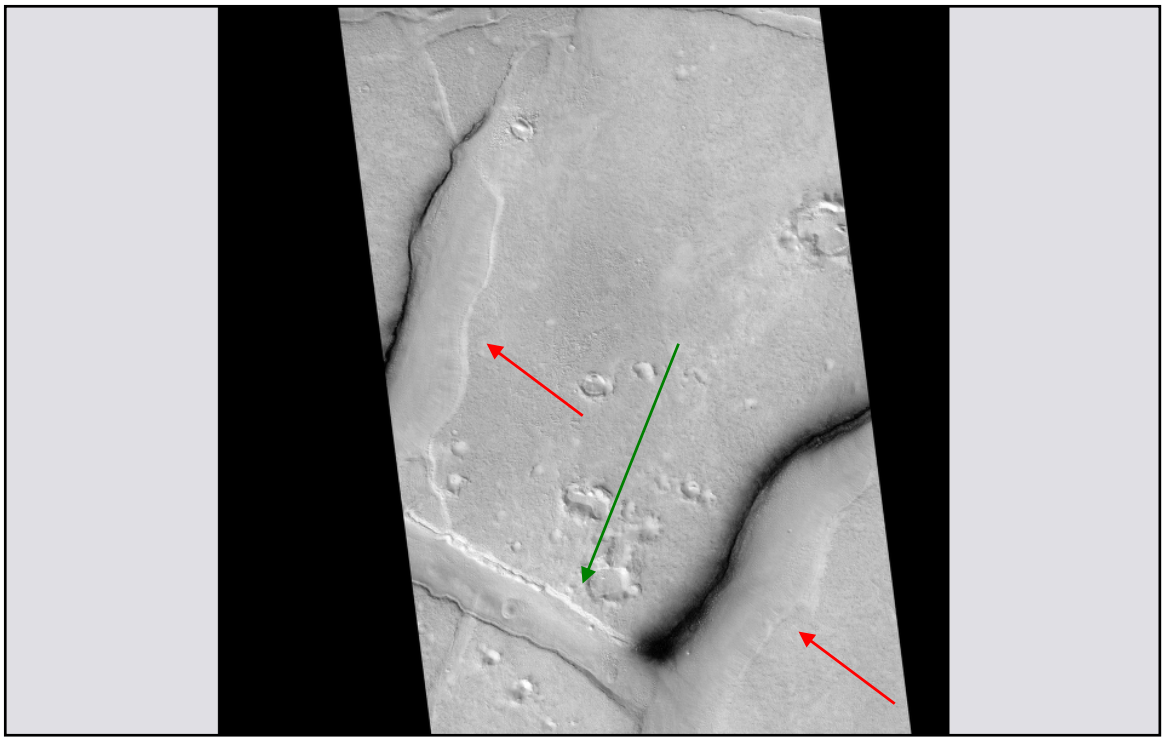

Figure 5: HiRISE image PSP6500_2200

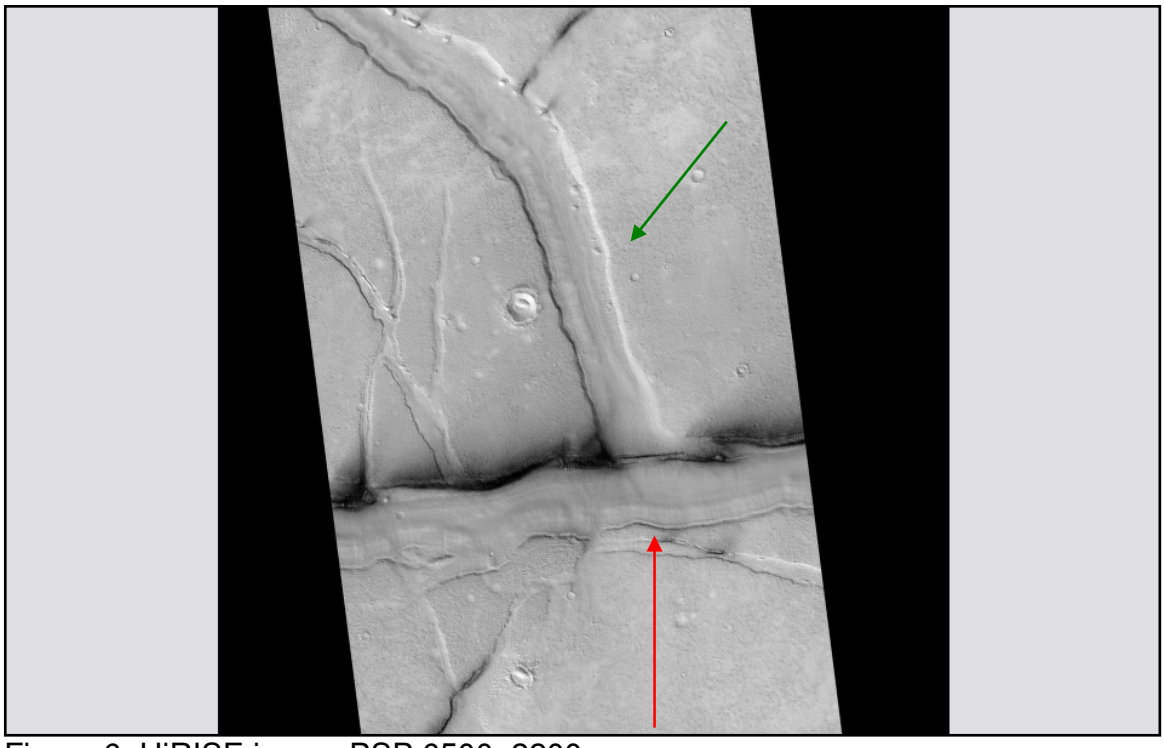

Figure 6: HiRISE image PSP 6500_2200

Running average of fault spacing

In addition to trough morphology, trough spacing with respect to the center of the Utopia basin was analyzed to determine if trough spacing relates to cover thickness. The center of the buried impact basin would have the greatest thickness of overlying sediments with progressively less material towards the edges. A 1-2 km thickness of buried material is expected in this area of the Utopia Basin [Scott and Tanaka, 1986; Buczkowski and Cooke, 2004]. Using a 100m/pixel resolution Thermal Emission Imaging System (THEMIS) Infrared Daytime image mosaic [Banfield, 2006] of Utopia, we measured surface trough spacing of the giant polygons along selected radial transects (Figure 7) from the center of the basin in the study area. In Figure 7, the numbered black lines are the transects and the white curvilinear line indicates a distance of ~550 km from the center of the basin. These transects were chosen based on an areal extent of polygonal terrain without significant influence of younger, large impact craters. Using the trough spacing measurements, a 3-point running average of trough spacing was created in order to investigate whether there is a relationship between the trough spacing and the layer within which the fault networks occur. Observations show running averages of trough spacing do not systematically decrease as a function of distance as would be expected if layer thickness controlled fault spacing. Examples of this are shown in Figure 8 for radial transects 4 and 5. The largest polygons are not observed beyond ~550 km from the center of the basin, however 5 of the 7 transects analyzed in this study show a non-monotonic change in fault spacing with smaller fault spacing closer to the center of the basin and larger fault spacing farther away from the center. This lack of monotonic decrease in

polygon spacing with distance from the basin center rules out a smooth basement beneath sedimentary material.

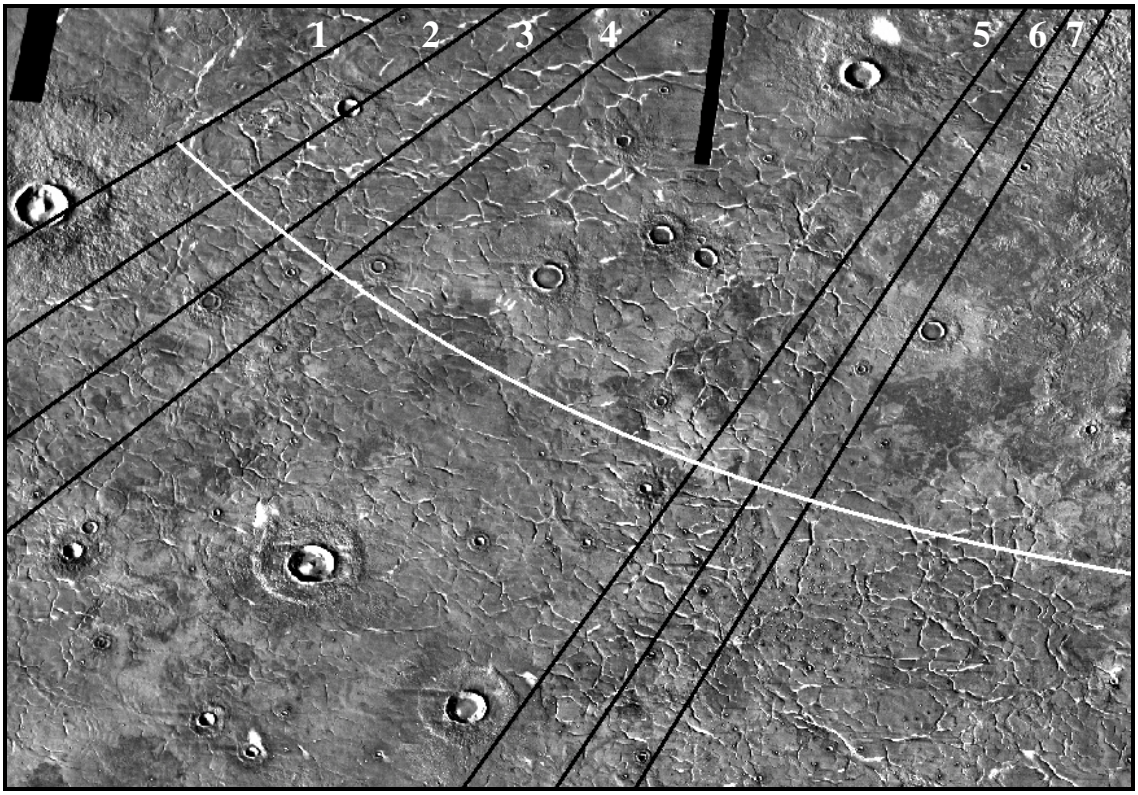

Figure 7: Black numbered lines are the radial transects and the white curvilinear line represents a distance of ~550km from the center of the basin.

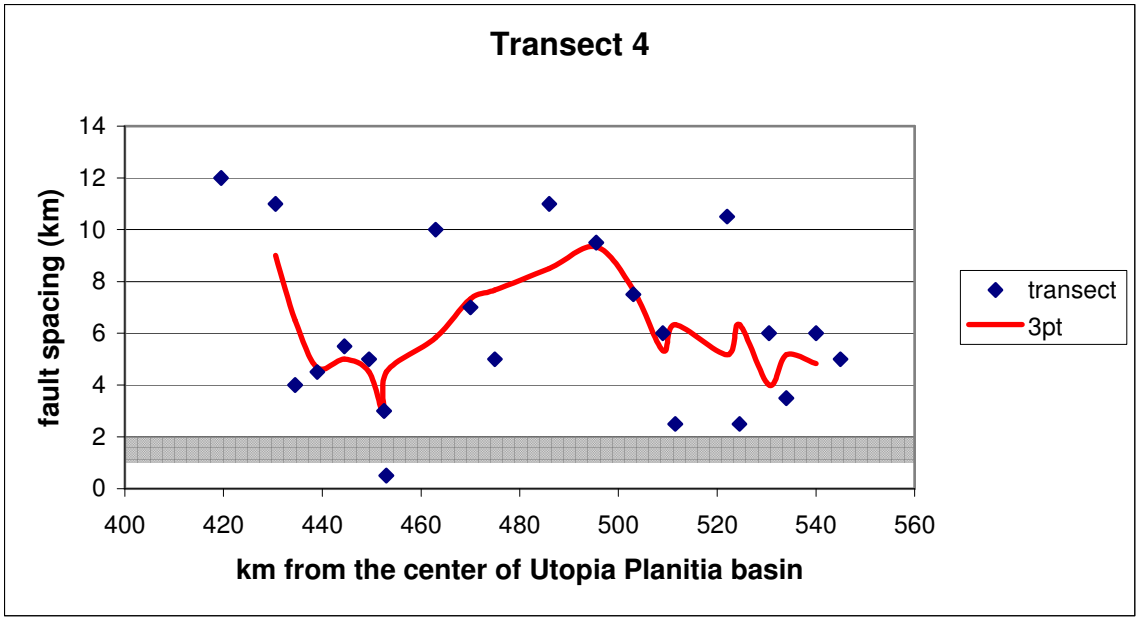

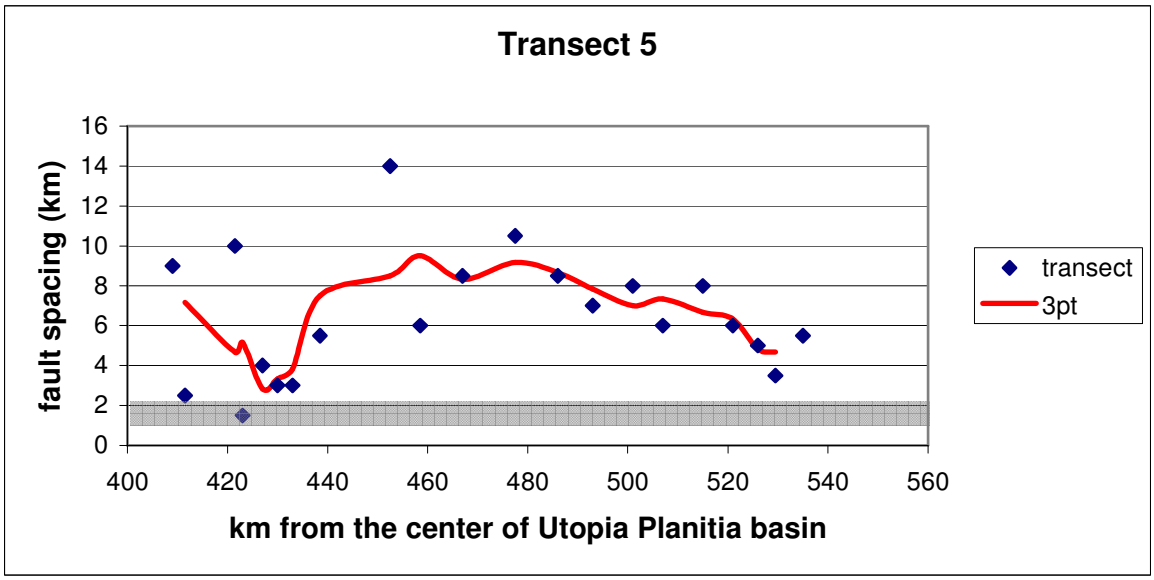

Figure 8: The red line is a 3 point running average of the intersected grabens along the transect which are shown as blue diamonds. The grey shaded rectangle represents the 1-2km thickness of material expected for this area of Utopia.

Average fault spacing in Utopia

We also measured average surface trough spacing of the giant polygons along the same radial transects. The average trough spacing ranges from 5 – 6.5 km, depending on the specific transect. North Sea polygons are layer-bound so fault spacing scales to layer thickness [Cartwright and Lonergan, 1996; Bai and Pollard, 2000]. If this were the case for the Utopia Basin, then fault spacing should be twice the layer thickness. 5-6.5 km average spacing of grabens implies a layer thickness of 2.5-3.35 km. This is greater than twice the 1-2 km layer thickness expected in this region of the Utopia Basin [Scott and Tanaka, 1986; Buczkowski and Cooke, 2004]. Consequently, basement topography, such as the buried slopes of craters, may act to initiate faults as the cover material compacts [Buczkowski and Cooke, 2004]. In this way, the spacing of polygons may reflect the spacing of the irregularities in the buried topography rather than depth of sedimentary material. The idea that the scale of the giant polygons is determined by the topography of the underlying surface was originally proposed by McGill and Hills [1992] and is further explored in this paper using numerical models.

MOLA topography

To investigate this hypothesis with numerical models, the probable nature of the buried basement topography was characterized. Earlier researchers have inferred that the underlying topography of the Northern Lowlands is similar to the topography of the older, Southern Highlands [McGill and Hills, 1992; Frey *et al*., 2002]. 30 MOLA tracks were selected from an arbitrarily chosen section of the Highlands (0-30S and 0-60W) to characterize the topography beneath Utopia. The chosen area was selected to represent an area of heavily cratered Highlands terrain without tectonic, volcanic or a large-scale

impact influences. 2800 consecutive points were sampled from each track and the measurements were approximately 300m apart, the horizontal spacing of the altimeter's measurements along each track. We measured the absolute value in the change in elevation from one shot point along the track to the next point and labeled this ΔH. Since the influence of any regional slopes measured for Mars is insignificant at the 300m scale, measuring ΔH gives only the magnitude of elevation changes over 300m. When ΔH values of the selected region of Highlands topography were binned into 5m intervals and plotted as a frequency histogram (Figure 9), the data best fit a power-law distribution. The power-law distribution of the Highlands topography indicates that frequent 5 to 15m scale elevation differences are observed at 300m spatial scale distances and very few 100m to 300m or larger elevation differences are recorded at the same scale. Of course there are elevation changes smaller than 5m recorded, however the vertical resolution limit of the altimeter is 5m, so measurements less than 5m were omitted from our analysis. Our results are consistent with other researchers who have observed the power-law distribution surface topography on Mars based on the analysis of MOLA tracks [Smith *et al*., 2000]. The power-law distribution of the topography is given by the formula:

$$Y = cx^{-k}$$

where x is raised to the power –k and c is a constant. The k value that best matches the change in elevation frequency distribution of the selected MOLA topography is -1.998.

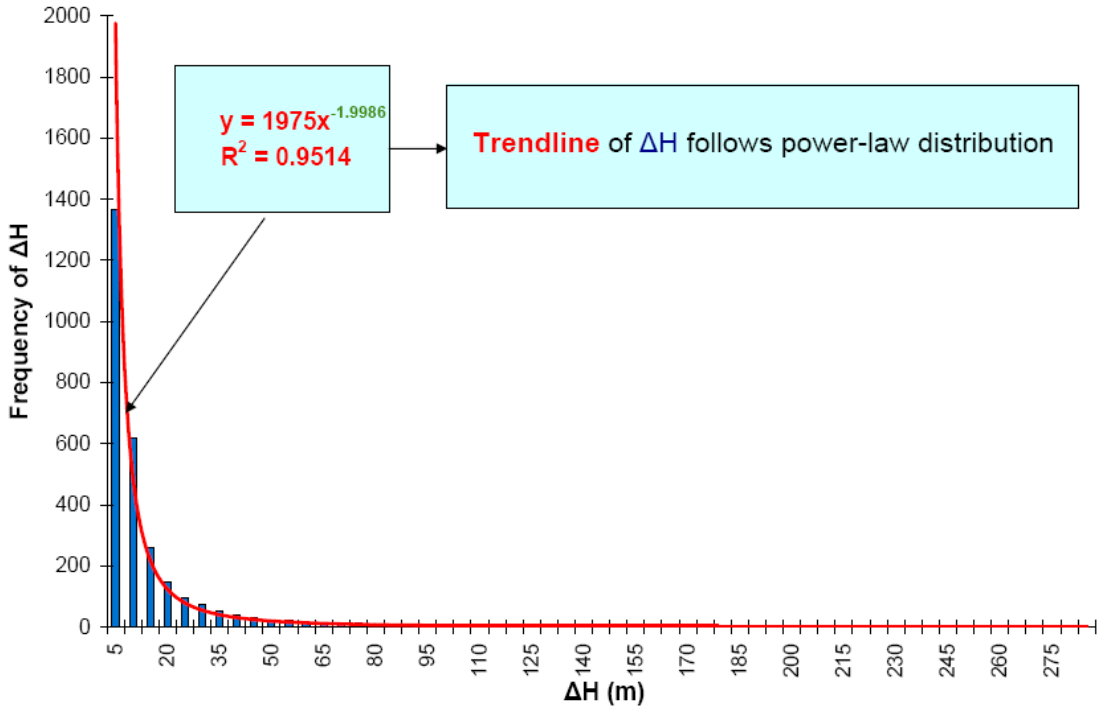

Figure 9: Power-law distribution of ΔH for the selected Highlands topography

CHAPTER 4

NUMERICAL MODEL OF THE UTOPIA BASIN

Introduction to the problem

In order to understand whether buried topography is controlling the trough spacing of the giant polygons, this study uses Boundary Element Method (BEM) numerical models to simulate the first-order mechanics of the faulting process. Models use material properties for wet, fine sediment analogous to the terrestrial counterpart and apply an extensional strain to simulate volumetric contraction. Fracture seeds that simulate the uneven topography beneath the basin are evenly placed at the base of the model. MOLA tracks from the Highlands are used to simulate the uneven topography beneath the basin. The model investigates whether 1 & 2 km thick layers of wet, fine sediments will produce the fracture spacing observed within the polygonal terrains in Utopia (~5 – 6.5 km).

Description of BEM

Numerical models can prescribe tractions or displacements along boundaries to determine stresses and strains throughout a body using continuum mechanics [e.g., Crouch and Starfield, 1990]. BEM is a particularly efficient numerical methodology, as only model boundaries and discontinuities (such as faults) need to be discretized. BEM is thus less computationally expensive than other numerical methods, such as Finite Element Method (FEM), which require discretization of the entire body.

The two-dimensional BEM code FRIC2D [Cooke and Pollard, 1997] applies the displacement discontinuity formulations of Crouch and Starfield [1990] to boundary elements of equal length. Each boundary element is assigned either traction or a

displacement in both the normal and shear directions. The code then can determine the displacements that result from a prescribed traction or the tractions that are necessary for a prescribed displacement, as well as the stresses and displacements throughout the body. The displacements remain constant along the length of each element, regardless of prescribed boundary conditions. Like many other BEM models, FRIC2D assumes that the host material is linear-elastic and homogeneous. In this study, we used FRIC2D to investigate the growth of extensional structures within cover material overlying an irregular substrate.

Model set-up

We set up two suites of models, 1 & 2 km in height and 50 km in length, to encompass typical diameters of the giant polygons (Figure 10). The top boundary of the model is a traction-free surface and the bottom boundary is frictionless. The left boundary is pinned and the right boundary is given horizontal displacement. Thus, the model deforms under horizontal extension, which simulates volumetric contraction. The Fric2D cross-sectional models use material properties for wet, fine sediment to simulate a water-laid depositional environment; we used Young's modulus of 48 MPa and a Poisson's ratio of 0.35.

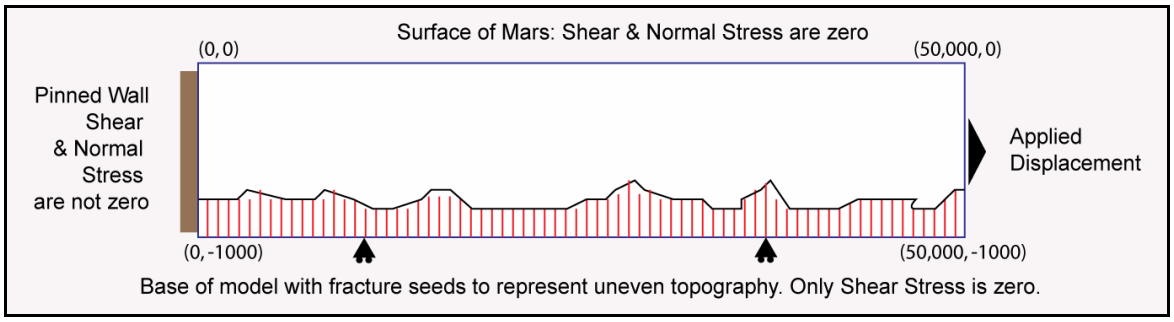

Figure 10: Not to scale conceptual sketch of the numerical model with boundary conditions and model dimensions. The red lines represent the fracture seeds used to simulate underlying topography.

These individual fractures grow by fracture propagation when the stress intensity at the fracture tip exceeds the fracture toughness of the material for an applied extensional strain. 500m of displacement is applied on the right wall in 10 steps at 50m increments (i.e. 50m displacement at step 1, 100m displacement at step 2 and 500m displacement at step 10). Within the model, fractures grow and propagate as opening-mode cracks. Although the grabens that form the polygonal terrain develop via pairs of normal faults that differ from the opening-mode fractures investigated here, the first order mechanics of propagation of both of these extensional structures are similar. The overall patterns of grabens can be matched within models comprised of opening mode fractures [Tuckwell *et al.*, 2003; Koenig and Pollard, 1998]. Consequently, the spacing of opening mode fractures that reach the upper surface of the model (Figure 11) can be compared to the spacing of troughs within the polygonal terrain on Mars.

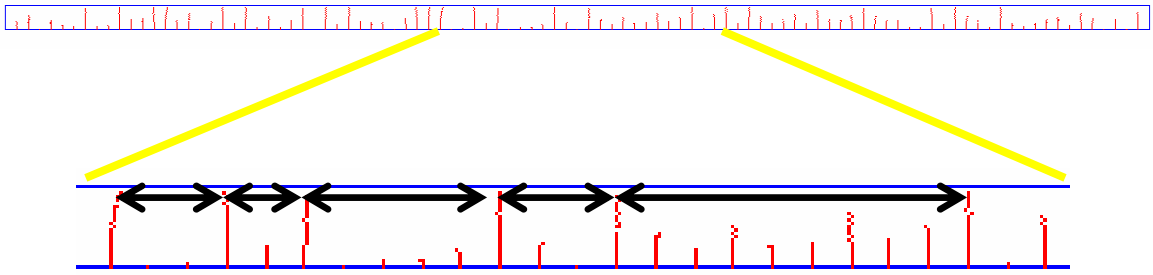

Figure 11: The top figure is the actual-scale 1 km by 50 km model at completion. The bottom figure is a magnified section of the model. The red lines are the fractures and the two-sided black arrows indicate the spacing between those fractures that have propagated to the top boundary of the model.

The power-law distribution of topography on Mars

There are 166 fracture seeds evenly placed 300m apart along the 50 km length of the model. The length of the fracture seeds within the model follow the power-law distribution of Highlands topography with many small-length fracture seeds (5-15m) and relatively few large-length fracture seeds (100m or larger). Each of the many monte-carlo realizations of fracture seed lengths follows the power-law distribution with k=-1.998, however, each realization is different from other realizations in the pattern of fracture seeds. Therefore, each realization of the model has a unique distribution of fracture seed lengths analogous to uniqueness of 2 adjacent MOLA tracks in the same terrain; the changes in elevation along each track are similar but never the same and similarly each realization follows a power-law distribution but is unique.

CHAPTER 5

COMPARISON OF MODEL RESULTS TO THE UTOPIA BASIN

1km & 2km models

80 realizations of the 1km model and 27 realizations of the 2km model were produced for this study. Table 1 shows the average fracture spacing of each realization at completion. The average surface fracture spacing for the 1km model is ~5km for realizations 51-80, on the order of the measured trough spacing in the Utopia Basin. For the 2 km model, realizations 51-60 and 63-80 produced ~7km average surface fracture spacing, 0.5km greater than the greatest average trough spacing measured along radial transects in Utopia. Figure 12 plots the average fracture spacing of all realizations for both suites of models against the percent applied strain at each step of the model. By the completion of the model, 1% applied strain has been applied. The 5-7km range of surface fracture spacing of both suites of models is in close agreement with the 5-6.5km measured trough spacing in the Utopia Basin shown as the gray shaded area in Figure 12. For both the 1 & 2 km models, the spacing is established by 0.6 to 0.7% strain and further strain does not significantly change the average fracture spacing as indicated by the negligible change in average surface fracture spacing from 0.7% strain to completion at 1% strain. If both suites of models exhibited large changes in fracture spacing at completion similar to spacing from 0.2% to 0.5% strain, then the results would not indicate that the fracture spacing has been established within the models and greater than 1% strains would be required.

Table 1: Fracture spacing and k for model realizations

Realization No.	Surface Fracture Spacing (km) 1km models	Surface Fracture Spacing (km) 2km models	k
1	1.471		-1.4693
2	4.545		-2.1323
3	6.25		-1.3254
4	5		-1.8559
5	4.545		-1.7798
6	2.083		-2.0392
7	4.167		-1.6082
8	3.571		-1.5738
9	2		-1.9321
10	2.083		-0.8262
11	2		-1.3127
12	2.273		-1.8858
13	2.083		-1.6769
14	5		-1.4716
15	2.632		-1.7787
16	3.846		-1.352
17	2.632		-1.2992
18	4.167		-2.0782
19	4.167		-1.4672
20	8.333		-1.815
21	10		-1.8245
22	4.167		-1.6281
23	4.545		-0.8446
24	5		-1.7923
25	2.174		-1.2886
26	12.5		-0.9806
27	5.556		-1.391
28	4.545		-1.7149
29	1.667		-2.0844
30	4.545		-1.7597
31	3.846		-2.3144
32	2.273		-1.2261
33	2.381		-1.5172
34	4.167		-2.1527
35	2.941		-1.2563
36	10		-0.8601
37	5		-1.8377

"continued on the next page"

38	4.545		-1.8954
39	1.724		-1.7
40	2		-1.4349
41	1.923		-2.1408
42	5		-1.4809
43	5.556		-1.8859
44	5		-1.336
45	7.143		-0.7437
46	2.632		-1.7338
47	7.143		-1.4023
48	4.545		-0.7386
49	5.556		-1.5758
50	6.25		-1.2647
51	3.846	7.14286	-1.6859
52	3.333	8.33333	-1.5187
53	2.273	4.54545	-1.9736
54	1.852	6.25	-1.9611
55	16.667	10	-2.1789
56	5	8.33333	-1.5771
57	5.556	7.14286	-1.6577
58	1.786	8.33333	-2.0124
59	7.143	7.14286	-1.6111
60	5	5.55556	-2.1233
61	5.556		-2.0836
62	10		-1.9579
63	5.556	7.14286	-1.5248
64	3.571	7.14286	-1.8986
65	8.333	7.14286	-1.8409
66	3.125	6.25	-1.6457
67	3.333	4.54545	-2.0282
68	2.5	8.33333	-1.5161
69	3.125	8.33333	-1.8099
70	2.381	8.33333	-1.8689
71	3.846	6.25	-1.5416
72	6.25	7.14286	-1.4544
73	8.333	10	-2.0565
74	3.125	8.33333	-1.7504
75	1.923	6.25	-2.1064
76	3.846	4.54545	-1.7972
77	8.333	5.55556	-1.7297
78	5.556	4.54545	-1.9155
79	6.25	6.25	-1.7806
80	2.381	7.14286	-2.0412

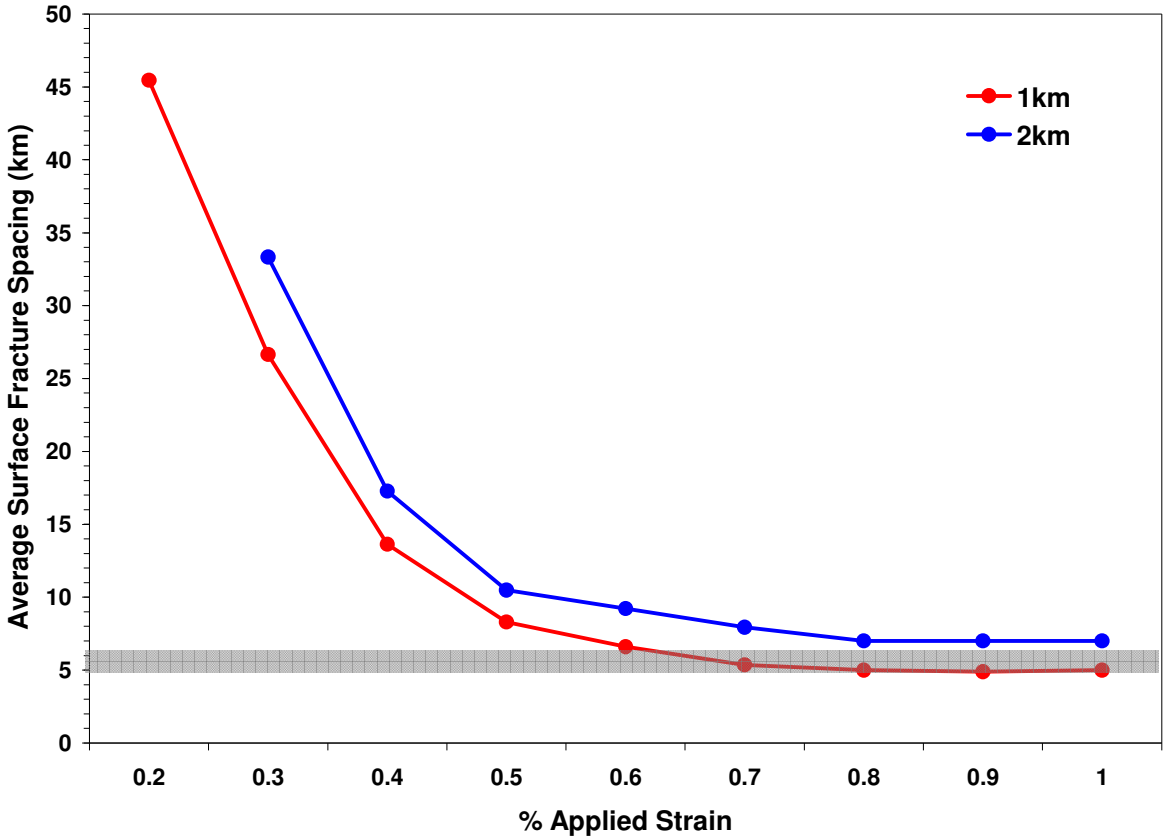

Figure 12: Graph of average surface fracture spacing at each step up to completion vs. % applied strain at each step for 1 & 2 km models. The red line is the 1 km model, the blue line is the 2 km model, and the gray shaded region is the observed average 5-6.5 km trough spacing in Utopia.

The power-law k

However, the model is sensitive to the k value derived from the power-law distribution of Highlands topography and subsequently used to create the fracture seeds. In Table 1, the last column lists the k value of each realization. The variability in k values (-0.7386 to -2.3144) is due to the comparatively smaller number of flaws per realization (166 pts) than the number of sampling points (30 tracks, 2800 pts per track) for Mars. For this reason, realizations 51 through 80 were selected to have k values closer to the

measured Highlands value of k = -1.998 and only realizations from this subset were used to produce the 2 km models.

Comparing fractures to faults

When the k value within the models more closely matched the observed value for the Highlands, the results indicate that relatively low strain (less than 1%) can create the scale of the troughs in the Utopia Basin. The low strain implies that buried topography may be the first-order control of the spacing of the grabens. Since the models create fractures, and the troughs in the polygonal terrain are grabens with displacement, further strain is not ruled out by model results. This study shows that the scale of the polygonal terrain is controlled by buried topography and further widening of the troughs can accommodate additional strain.

CHAPTER 6

DISCUSSION

Sensitivity of models to k

Buried basement slopes wider than 300m such as the inner wall to the center of large crater are likely under the cover material. If we only sample changes in elevation at 300m intervals along MOLA tracks, then we will not sample larger scale elevation differences and this would incorrectly characterize the topography. In order to test sampling effects, we rebinned 10 of the 30 MOLA tracks used in this study at the 600m and 1200m scale to see if this produces a different power-law distribution. Instead of noting the change in elevation from one point to the next, we also sampled every other point and every fourth point. At both scales, the data still followed a power-law distribution, but each scale doubling lowered the k. For 300m, the average k=-1.998, for 600m, k=-1.79, and for 1200m, k=-1.59. This range of k is represented in the 80 realizations, and the variability of the larger sampling intervals is less than the models variability in k as explained earlier.

Figure 13 shows average surface fracture spacing for all realizations of the model plotted against the k value for each realization. For most models, fracture spacing is greater than double the layer thickness (~2km or greater average surface fracture spacing for the 1km model and ~4km or greater average surface fracture spacing for the 2km model). The wide range of k values does not significantly affect the average surface fracture spacing for the 1 or 2 km models.

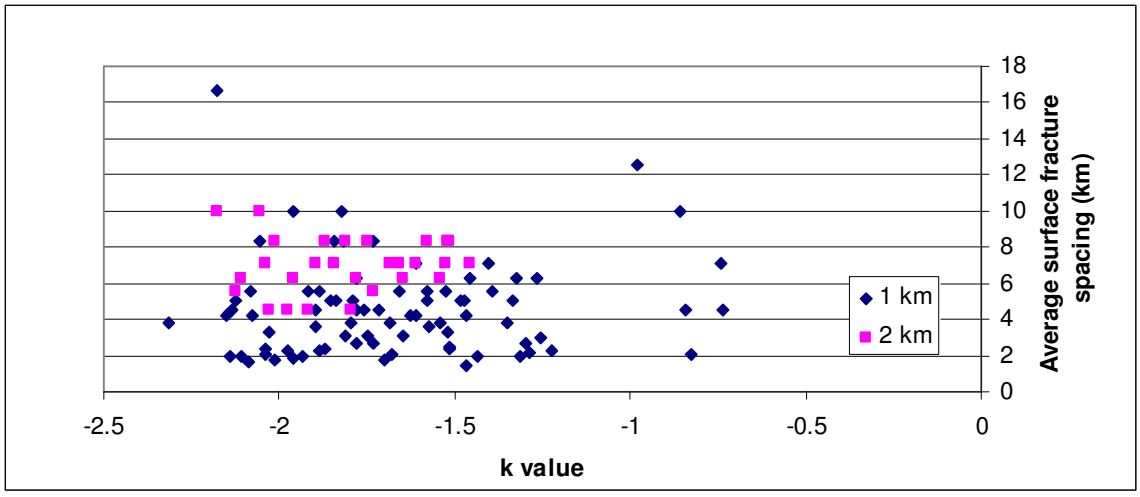

Figure 13: 1 & 2 km model realization spacing vs. k for the given realization

Role of stiffness in model fracture spacing

A Young's modulus for fine, unconsolidated sediments (48 MPa), analogous to the strength of the mudrocks that form the terrestrial sedimentary basin polygons, yields Mars scale fracture spacing within the model. The model's stiffness does play a factor in fracture spacing. Fischer et al., [1995] among others have shown that a stiff layered medium produces smaller stress shadows around cracks than a softer layered medium and therefore has smaller joint spacing than the softer layer. For our results, this implies that a mechanically stronger material such as consolidated mudrocks or sandstone would produce more surface fractures within our models for the same power-law fracture seed distribution. Since buried topography is the first-order control on the model and has the strongest influence on spacing, the sensitivity of the model to the strength of material has not been explored further in this study.

CHAPTER 7

CONCLUSIONS

A fracture network that is similar to the scale of the polygonal terrain in the Utopia Basin is established within our model at low strain, supporting the idea that buried topography could be the primary scaling factor for the polygon grabens. The results do not constrain an upper limit for strain; the observed trough widths suggest that further strain was expressed by the widening of the troughs. Material properties for wet, fine sediments, analogous to the terrestrial counterpart, are appropriate for the model to match what is observed in Utopia. Materials that are stiffer and more consolidated would produce more fractures for the same power-law distribution of initial flaws in our model and therefore would not match what is observed. A smooth basement with no buried topography would yield a monotonic decrease in trough spacing along radial transects with respect to the center of the basin and this is also not observed in our study. The power-law scale of Highlands topography controls the scale of the fracture spacing in our models. Therefore our results show that this may be the case for the polygonal terrain of Utopia Planitia, Mars.

BIBLIOGRAPHY

Aharonson, O., Zuber, M.T. and Neumann, G.A., Mars: Northern hemisphere slopes and slope distributions, *Geophys. Res. Lett*., 25(24), 4413-4416, 1998.

Bai, T. and Pollard, D. D., Fracture spacing in layered rocks: a new explanation based on the stress transition, *J. Struct. Geol.*, 22, 43–57, 2000.

Banfield, J., THEMIS Daytime Infrared Mosaic, Arizona State University, 2006.

Buczkowski, D.L. and Cooke, M.L., Formation of double-ring circular grabens due to volumetric compaction over buried impact craters: Implications for thickness and nature of cover material in Utopia Planitia, Mars, *J. Geophys. Res.*, 109, E02006, 2004.

Cartwright, J.A., Episodic basin-wide fluid expulsion from geopressured shale in the North Sea basin, *Geology*, 22, 447-450, 1994.

Cartwright, J.A. and Dewhurst, D.N., Global distribution of layer-bound compaction faults, *Geol. Soc. Am. Bull*., 110(10), 1242–1257, 1998.

Cartwright, J.A. and Lonergan, L., Seismic expression of layer-bound fault systems of the Eromanga and North Sea Basins, *Expl. Geophys*., 28, 323–331,1997.

Cartwright, J.A. and Lonergan, L., Volumetric contraction during the compaction of mudrocks: a mechanism for the development of regional-scale polygonal fault systems, *Basin Res.*, 8, 183–193, 1996.

Cooke, M.L. and Pollard, D.D., Bedding-plane slip in initial stages of fault-related folding, *J. Struct. Geol*., 19, 567-581, 1997.

Crouch, S.L. and Starfield, A.M., *Boundary Element Methods in Solid Mechanics*, 322 pp., Chapman and Hall, New York, 1990.

Dewhurst, D.N., Cartwright, J.A. and Lonergan, L., The development of polygonal fault systems by syneresis of colloidal sediments, *Mar. Petr. Geol.*, 16, 793–810, 1999.

Fischer, M.P., *et al*., Finite-element analysis of the stress distribution around a pressurized crack in a layered elastic medium: implications for the spacing of fluid-driven joints in bedded sedimentary rock, *Tectonophysics*, 247, 49-64, 1995.

Frey, H.V. et al., Ancient lowlands on Mars, *Geophys. Res. Lett.,* 29(10), 1384, 2002.

Gay, A., Lopez, M., Cochonatz, P. and Sermondadaz, G., Polygonal faults-furrows system related to early stages of compaction; upper Miocene to recent sediments of the Lower Congo Basin, *Basin Research***,** 16(1), 101-116, 2004.

Hiesinger, H. and Head, J.W., Characteristics and origin of polygonal terrain in southern Utopia Planitia, Mars: Results from Mars Orbiter Laser Altimeter and Mars Orbiter Camera data, *J. Geophys. Res.*, 105, 11,999-12,022, 2000.

Koenig, E. and Pollard, D.D., Mapping and modeling of radial fracture patterns on Venus, *J. Geophys. Res.,* 103, 15,183-15,202, 1998.

Lonergan, L., Cartwright, J., and Jolly, R., The geometry of polygonal fault systems in Tertiary mudrocks of the North Sea, *J. Struct. Geol*., 20(5), 529–548, 1998.

Lucchitta, B.K., Ferguson, H.M. and Summers, C., Sedimentary deposits in the northern lowland plains, Mars, *J. Geophys. Res*., 91, suppl., E166-E174, 1986.

McGill, G.E., Buried topography of Utopia, Mars: Persistence of a giant impact depression, *J. Geophys. Res*., 94, 2753-2759, 1989.

McGill, G.E. and Hills, L.S., Origin of giant martian polygons, *J. Geophys. Res*., 97, 2633-2647, 1992.

Mouginis-Mark, P.J., Martian fluidized crater morphology; variations with crater size, latitude, altitude, and target material, *J. Geophys. Res.*, 84, 8011-8022, 1979.

Pechmann, J.C., The origin of polygonal troughs on the northern plains of Mars, *Icarus,* 42, 185-210, 1980.

Thompson, B.J. and Head, J.W., Utopia Basin, Mars: A new assessment using Mars Orbiter Laser Altimeter (MOLA) data, In *Lunar and Planetary Science XXX*, Abs. #1894, Lunar and Planetary Institute, Houston (CD-ROM), 1999.

Scott, D.H. and Tanaka, K.L., Geologic map of the western equatorial region of Mars, *U.S. Geol. Surv. Misc. Invest. Ser.*, Map I-1802-A, 1986.

Smith, D.E. et al., The global topography of Mars and implications for surface evolution, *Science*, 284, 1495-1503, 1999.

Smith, D.E., *et al*., Mars Orbiter Laser Altimeter: Experiment summary after the first year of global mapping of Mars, *J. Geophys. Res*., 106(E10), 23,689–23,722, 2001.

Tuckwell, G.W., Lonergan, L. and Jolly, R.J.H., The control of stress history and flaw distribution on the evolution of polygonal fracture networks, *J. Struct. Geol*., 25, 1241–1250, 2003.